

# Multi-Objective Optimization Design of the Ejector Plate for Rear-Loader Garbage Trucks

Fu-sheng Ding<sup>1</sup> – Hong-ming Lyu<sup>1</sup> ✉ – Jun Chen<sup>2</sup> – Hao-ran Cao<sup>1</sup> – Lan-xiang Zhang<sup>1</sup>

<sup>1</sup> Yancheng Institute of Technology, School of Automotive Engineering, China

<sup>2</sup> Jiangsu Yueda Special Vehicle Co., Ltd., China

✉ hongming\_lyu@ycit.edu.cn

**Abstract** This work presents a multi-objective optimization design approach for the ejector plate, a critical component of rear-loader garbage trucks, with the goal of ensuring structural integrity and optimizing lightweight performance. A parametric finite element model of the ejector plate is developed with optimization objectives focused on minimizing mass, controlling deformation, and reducing the maximum von Mises stress. Through sensitivity analysis, seven key variables are selected for optimization. A Box-Behnken design (BBD) is used to systematically explore these parameters, and a Kriging surrogate model is constructed to approximate the objective function, with accuracy benchmarked against response surface methodology (RSM). The Non-dominated Sorting Genetic Algorithm II (NSGA-II) is applied to derive the optimal solution, achieving a lightweight design meeting all structural requirements. The results show that the mass of the ejector plate of the rear-loading waste compactor can be reduced by 6.06 % through structural optimization, while meeting the strength and deformation criteria. This improvement not only enhances waste transportation efficiency, but also lowers production costs and enhances material utilization.

**Keywords** garbage truck, ejector plate, multi-objective optimization, NSGA-II, Kriging

## Highlights

- Optimizing the ejector plate considering the mass, maximum displacement and maximum von Mises stress of the ejector plate.
- Using sensitivity analysis to identify key design variables of the ejector plate.
- Using Kriging method to construct a highly accurate surrogate model.
- Applying the non-dominated sorting genetic algorithm II for multi-objective optimization of the ejector plate.

## 1 INTRODUCTION

As the global economy grows and urbanization accelerates, the generation of household waste has increased significantly. This trend is putting immense pressure on urban environmental health and poses challenges for sustainable urban development [1]. Given the substantial volume of urban waste, efficient transportation and disposal methods have become critical concerns for municipalities and related departments [2]. Rear loader garbage trucks are specialized vehicles designed to operate with waste compaction transfer stations. Their widespread adoption by sanitation and municipal departments can be attributed to their large loading capacity and effective sealing. The ejector plate, a key component of these trucks, plays a vital role in the loading and unloading of waste. Different types of waste impose varying demands on the strength of the ejector plate. During the compaction and loading/unloading processes, the ejector plate is subjected to forces from both the hydraulic cylinder and the waste itself, resulting in varying degrees of deformation. Such deformation can reduce the compaction ratio within the truck's box body, ultimately diminishing loading and unloading efficiency and affecting the truck's overall waste capacity. Therefore, research into the ejector plate is crucial for the effective design of garbage trucks.

The three dimensional (3D) model of the ejector plate was developed in SolidWorks software, which was then subjected to finite element analysis (FEA) to evaluate its stress and displacement distributions under operational conditions [3]. The garbage truck loading mechanism served as the research focus, with parametric analysis conducted to establish the functional relationships among compression-filling force, pusher stroke, and installation angle [4]. The garbage truck manipulator was digitally prototyped in SolidWorks for performance enhancement, followed by a multi-

domain simulation workflow: multi-body dynamic (MBD) analysis in ADAMS determined operational load spectra under various working conditions, FEA in HyperWorks assessed structural integrity, and topology optimization integrated with genetic algorithms achieved 16.73 % mass reduction while maintaining mechanical performance [5].

Lightweighting vehicles is an essential strategy for saving energy and reducing emissions [6,7]. Reducing the weight of vehicles can reduce energy consumption while improving dynamics and braking performance [8,9]. The main approaches to lightweight design include structural optimization, process optimization and material lightweighting [10-12]. Structural optimization can be further categorized into size optimization, shape optimization, and topology optimization [13]. Currently, size and shape optimization are widely used in engineering applications [14,15]. Size optimization can be divided into discrete and continuous categories based on the continuity of design variables. Continuous size optimization results typically require rounding to fit available size parameters, making discrete size optimization more suitable for practical project needs [16]. Furthermore, discrete optimization allows for the simultaneous optimization of multiple variables, potentially yielding superior results.

In the realm of optimal design algorithms, Goldberg was the first to apply genetic algorithms (GA) to multi-objective optimization in 1989 [17]. Subsequent research has built upon this foundation. For instance, Paz et al. [18] utilized multivariate adaptive regression spline techniques combined with multi-objective genetic algorithms to enhance the energy absorption properties of automotive components while reducing mass. Velea et al. [19] conducted multi-objective optimization of a composite body for electric vehicles, considering weight, cost, and stiffness. Duan et al. [20]

applied a multi-objective particle swarm optimization algorithm for lightweight design of body-in-white structures to meet reliability requirements. Jiang et al [21] employed the Kriging surrogate model alongside the non-dominated sorting genetic algorithm II (NSGA-II) for the multi-objective optimal design of suspension arms and torsion beams, achieving weight reduction without compromising structural or vehicle performance. Xie et al. [22] implemented a multi-objective optimization method incorporating the TOPSIS method for the lightweight design of commercial vehicle cabs, successfully meeting design requirements while achieving weight reduction.

The lightweight design of the ejector plate is directly related to the load capacity and reliability of the garbage truck. Therefore, pursuing a lightweight design for the ejector plate while considering both structural performance and load capacity is essential. This paper focuses on the ejector plate of a specific garbage truck, utilizing 3D design software for parametric modeling and conducting finite element analysis based on actual working conditions. A sensitivity analysis of mass, displacement, and equivalent force concerning fourteen key parameters is performed, identifying 7 parameters with greater sensitivity as design variables. These variables are then optimized using a combination of the Kriging surrogate model and the NSGA-II algorithm to achieve the lightweight design of the ejector plate.

## 2 METHODS AND MATERIALS

### 2.1 Working Principle of the Ejector Plate

As shown in Fig. 1, the rear loader garbage truck consists primarily of several components, including the vehicle chassis, box body, hydraulic cylinder, packing mechanism, and ejector plate, as illustrated in Fig. 2. The box body is mounted on and rigidly connected to the chassis frame. At the rear of the truck, the packing mechanism is responsible for loading and initially compacting the waste. The waste is then pushed into the box body by the action of a scraper on the packing mechanism. After each compaction, both the compacted waste and the newly loaded waste are gradually pushed toward the rear of the box body, with the ejector plate continuously moving back as new waste is added.

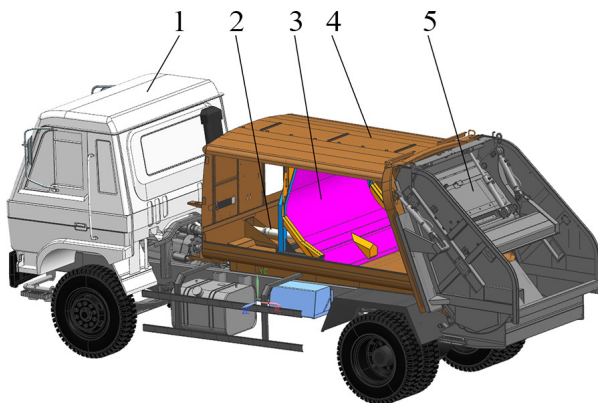


Fig. 1. Construction of the rear-loader garbage truck; 1 chassis, 2 cylinder 3 ejector plate, 4 box body, and 5 precompressor

### 2.2 Design Requirements for the Ejector Plate

The ejector plate consists of the front plate, frame skeleton, guide rail skeleton, cylinder support, and other components. As a critical load-bearing element of rear-loader garbage trucks, the mechanical properties of the ejector plate significantly impact the overall

performance of the vehicle. During operation, the ejector plate experiences the combined effects of hydraulic cylinder thrust, friction between the ejector plate and the guide rail, and the extrusion pressure from the refuse. The deformation of the ejector plate skeleton directly affects the gap between the ejector plate and the cargo area, which, in turn, influences the complete discharge of the waste.

Therefore, the design of the ejector plate must ensure that the deformation of the frame skeleton remains below 10 mm. In addition, under maximum external load conditions, the stress on all components should not exceed 355 MPa. To meet the performance requirements, the design of the ejector plate should also prioritize minimizing weight and maintaining high quality.

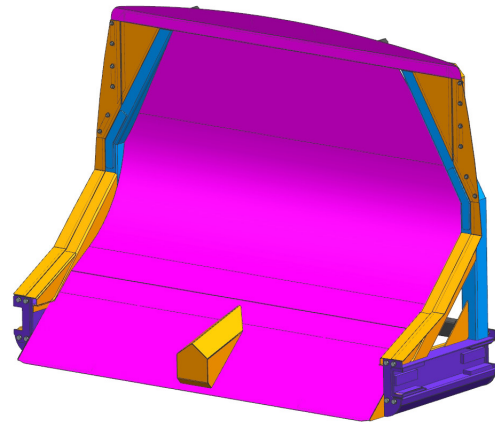


Fig. 2. 3D model of the ejector plate

### 2.3 Optimization Flow for the Ejector plate

This study employs a combination of the finite element method (FEM), Kriging Surrogate Model, and GA for optimization. The finite element method is utilized to calculate the maximum working load conditions of the ejector plate. Based on the results of the finite element analysis, a lightweight multi-objective structural optimization program is proposed which focuses on minimizing the total deformation, mass and von Mises stress. The Kriging surrogate model is known for its high accuracy, adaptability and scalability, making it widely applicable in the structural optimization design of various mechanical components [23,24]. Genetic algorithms are favored for multi-objective optimization due to their broad adaptability, global search capability, parallelism, and independence from derivative information [25]. The optimization process is illustrated in Fig. 3.

The specific steps are as follows:

- Parametric modeling: The ejector plate is modeled parametrically in 3D modeling software, and its finite element model is created in HyperWorks software, followed by static analysis.
- Sensitivity analysis: 14 parameters within the ejector plate skeleton are analyzed for sensitivity, leading to the selection of 7 parameters that significantly influence the mass, total displacement, and von Mises stress of the ejector plate skeleton for further analysis.
- Experimental design: The 7 highly sensitive parameters are sampled and tested using the Box-Behnken experimental design method.
- Surrogate model generation: A Kriging surrogate model is developed based on the experimental design parameters.
- Optimization: A multi-objective genetic algorithm (NSGA-II) is employed to obtain the optimal set of solutions and to validate the appropriateness of the selected optimization parameters.

## 2.4 Finite Element Analysis of the Ejector plate

### 2.4.1 Finite Element Model

When modeling, capturing the essence of the research object and appropriately simplifying the original model are essential for improving simulation efficiency and quality. The rubber buffer blocks on the ejector plate, and the sealing plates on both sides serve auxiliary roles that have minimal impact on the forces in the model, allowing them to be omitted from the modeling process.

The focus is on the overall structural characteristics of the ejector plate rather than localized welding issues. Rigid units are employed to simulate the weld relationships between different components, facilitating the transfer of forces. This simplified approach enhances the fidelity of the finite element results while significantly improving solution speed, enabling a more efficient design process that can accommodate a large number of experimental simulations.

In the ejector plate assembly, the cylinder support is a casting and is simulated using 8 nodes hexahedron elements. The other components are sheet metal parts, characterized by smaller dimensions in the thickness direction and larger dimensions in length and width, and are simulated using 4 nodes shell elements. Considering the enterprise's specifications for mesh size, as well as the need to maintain computational accuracy while minimizing computational cost, an 8 mm mesh was adopted for the model. Upon completing the meshing of the ejector plate, the model consists of 117,823 nodes and 117,117 elements, as shown in Fig. 4.

The material of the ejector plate is high-quality structural carbon steel (Q355B), with properties including a Young's modulus of  $2.1 \times$

105 MPa, a density of  $7850 \text{ kg/m}^3$ , and a Poisson's ratio of 0.3, and a minimum yield strength of 355 MPa.

As one of the primary load-bearing components of the truck, the ejector plate is subjected to the thrust from the hydraulic cylinder, the force exerted by the waste on its front plate during loading, and the support force from the guide rail. Due to the considerable stroke length of the ejector plate, a multi-stage hydraulic cylinder is employed; the shorter the stroke of the hydraulic cylinder, the greater the thrust produced. According to the hydraulic cylinder's operating behavior, the ejector plate experiences the greatest load and deformation when the truck is nearly full of waste and the ejector plate is close to its innermost position within the box body.

The hydraulic system operates at a pressure of 17.6 MPa. The ejector plate cylinder is a 3-stages rod cylinder, with the diameters of the rods measuring 90 mm (1<sup>st</sup> stage), 70 mm (2<sup>nd</sup> stage), and 50 mm (3<sup>rd</sup> stage). The maximum thrusts exerted by these rod sections are calculated to be 111.9 kN, 67.7 kN, and 34.5 kN, respectively. When waste is loaded into the box body, the force exerted by the waste on the ejector plate must overcome both the hydraulic cylinder's force and the friction between the ejector plate and the guide rail before the ejector plate can move inward. Thus, the ejector plate experiences maximum load when the hydraulic cylinder's thrust is 111.9 kN. The ejector plate moves slowly within the box body, neglecting the effects of dynamic loading. The friction force, which cannot be directly measured, is assumed to be approximately 12 kN (about 10 % of the maximum thrust). During slow movement, the force from the waste on the front plate is balanced by the hydraulic cylinder's force and

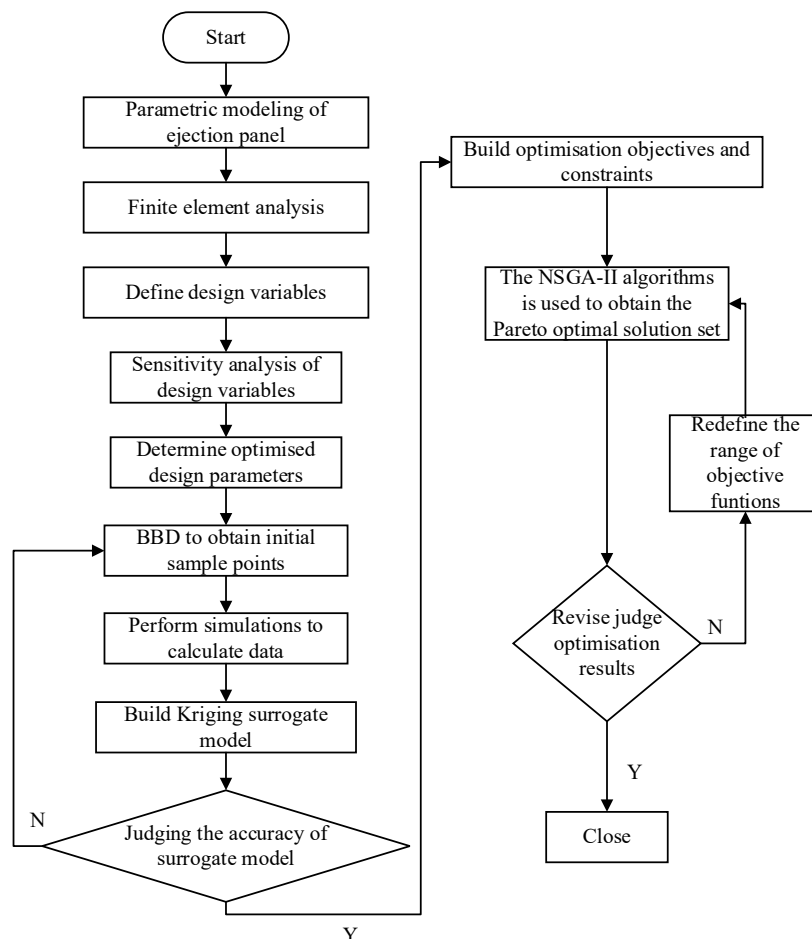


Fig. 3. Flow chart for optimization of the ejector plate structure

the friction between the ejector plate and the guide rail, resulting in a pressure of 0.06 MPa acting on the front plate.

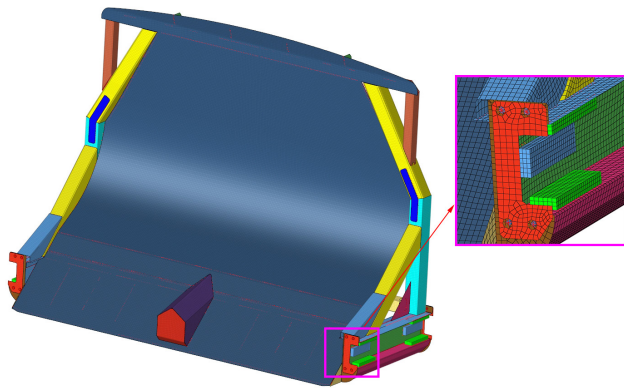


Fig. 4. Mesh model of the ejector plate

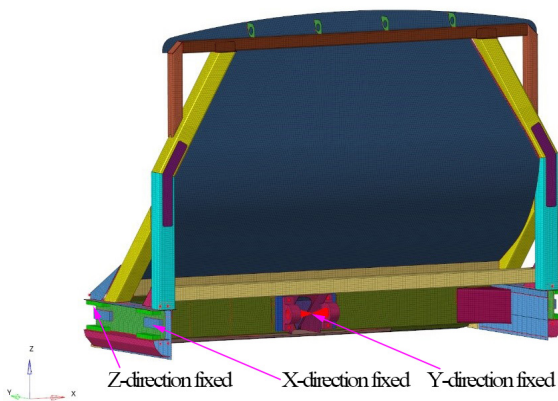


Fig. 5. Constraints of the ejector plate

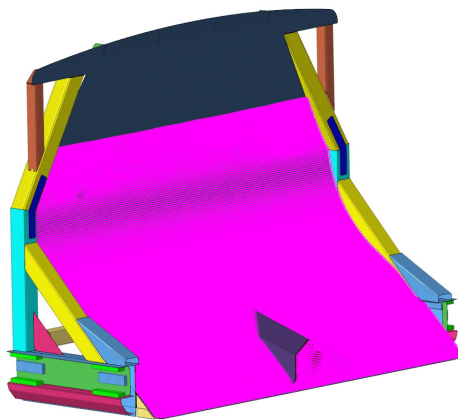


Fig. 6. Distribution of the load on ejector plate

In accordance with actual working conditions, fixed displacement constraints in the  $y$ -direction (forward and backward) are applied at the cylinder support of the ejector plate. Displacement constraints in the  $x$ -direction (left and right) are applied to the lateral friction blocks of the ejector plate guide, and  $z$ -direction (vertical) displacement constraints are applied to the upper and lower friction blocks of the guide, as shown in Fig. 5. A uniform compressive pressure load of 0.06 MPa is applied to the side of the front plate in contact with the waste. Considering that the waste cannot be loaded to the top of the box body, this load is applied only up to a height of 960 mm from the bottom plate, as illustrated in Fig. 6.

Taking into account the working conditions of the ejector plate, overload protection, personnel protection, material properties, etc., a safety factor of 1 is selected, and the allowable stress of the material is 355 MPa.

### 2.4.2 FEA Result Analysis

The finite element analysis yields to the static deformation and von Mises stress contours for the ejector plate and its skeleton, as illustrated in Fig. 7 through Fig. 10.

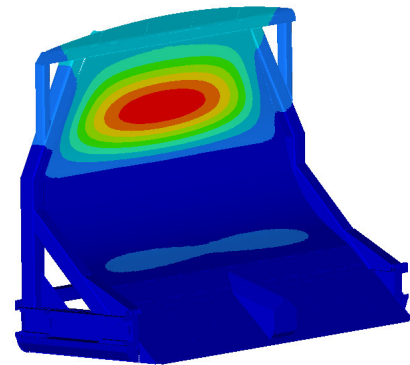
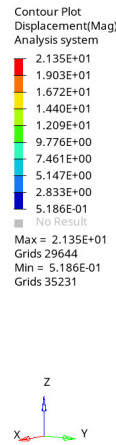


Fig. 7. Static deformation of the ejector plate



Fig. 8. Static deformation of the ejector plate skeleton

As shown in Fig. 7, the maximum deformation of the ejector plate is approximately 21.4 mm, which occurs in the central and upper areas of the front plate. This deformation corresponds to the actual working conditions. The ejector plate has a width of 1800 mm and the front plate is made of a 2.3mm thick steel plate. Although this design results in a relatively low stiffness, the significant deformation of the front plate does not affect its performance, provided that the deformation of the ram skeleton remains within acceptable limits.

Figure 8 indicates that the maximum deformation of the ejector plate skeleton is approximately 7.36 mm, concentrated in the middle of the upper tube, with progressively smaller deformations further down. This deformation is within the allowable limit of 10 mm specified in the design, demonstrating that the current ejector plate meets the stiffness requirements and possesses a degree of stiffness redundancy.

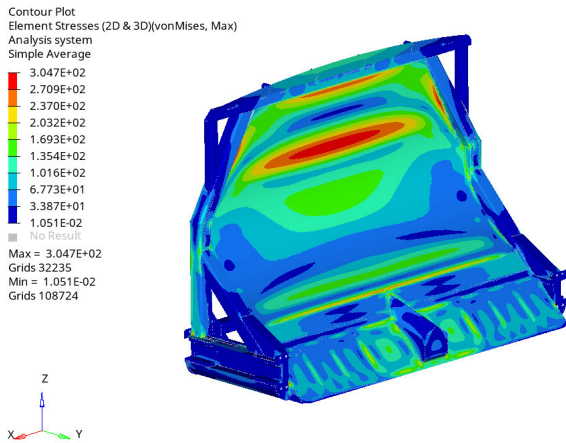


Fig. 9. von Mises stress distribution in the ejector plate

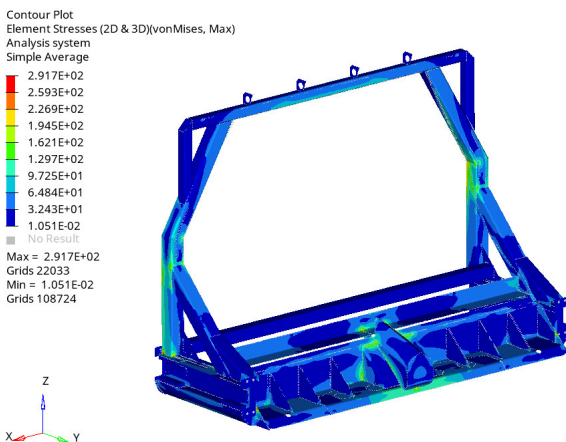


Fig. 10. von Mises stress distribution in the ejector plate skeleton

From Figure 9, it can be seen that the maximum von Mises stress of the ejector plate is 304.7 MPa, which is located in the middle and upper sections of the front plate.

In Figure 10, the von Mises stress contour for the ejector plate skeleton shows a maximum stress of 292 MPa, which is located in the lower sections of the side tube and below the design allowable stress limit of 355MPa.

To address the potential influence of mesh size on the simulation results, a systematic mesh sensitivity study was carried out specifically on the side tube (identified as the critical region with the highest stress concentration). Three different mesh configurations were tested: 8 mm, 6 mm, and 4 mm average element size. The corresponding results are summarized in Table 1 below.

Table 1. Mesh sensitivity analysis for the side tube

Mesh size [mm]	8	6	4
Max stress [MPa]	291.7	295.5	296.9
Stress increment [MPa]	-	+3.8	+5.2
Maximum stress difference	-	+1.3 %	+1.8 %
Number of side tube elements	2760	4450	9905

From Table 1, it can be seen that as the mesh is refined from 8 mm to 4 mm, the maximum stress exhibits a monotonic but diminishing increase, with a total variation of 1.8 % (5.2 MPa absolute difference), and the number of side tube elements shows an increase in geometric multiples, with a total variation of 258.9 % (7145 elements difference). The relative stress change between

successive refinements (6 mm vs. 8 mm: 1.3 %; 4 mm vs. 6 mm: 0.5 %) demonstrates convergence behavior, indicating that further mesh refinement beyond 6mm yields marginal improvements in accuracy. The sub-2% discrepancy between the 8 mm and 4 mm meshes falls within typical engineering tolerance thresholds for such analyses [26], confirming that the 8 mm mesh provides sufficient accuracy while maintaining computational efficiency.

The results of finite element analysis indicates that the current ejector plate skeleton meets the strength requirements and has a significant material surplus, allowing for potential lightweighting studies of the ejector plate structure.

## 2.5 Sensitivity analysis

### 2.5.1 Determination of Design Variables and objective functions

According to the structural characteristics and the stress distribution of the ejector plate's skeleton, the upper tube thickness  $P_1$ , reinforced tube I thickness  $P_2$ , side tube thickness  $P_3$ , side steel tube thickness  $P_4$ , angle iron thickness  $P_5$ , bracket thickness  $P_6$ , bottom skeleton thickness  $P_7$ , reinforced tube II thickness  $P_8$ , reinforced steel tube thickness  $P_9$ , angle brace thickness  $P_{10}$ , bottom plate thickness  $P_{11}$ , rail angle brace plate thickness  $P_{12}$ , rail skeleton thickness  $P_{13}$ , and rail support plate thickness  $P_{14}$  are used as the candidate design variables. The maximum static deformation  $D$ , maximum von Mises stress  $S$ , and mass  $M$  are used as objective functions. The position of each design variable of the ejector plate's skeleton is shown in Fig. 11.

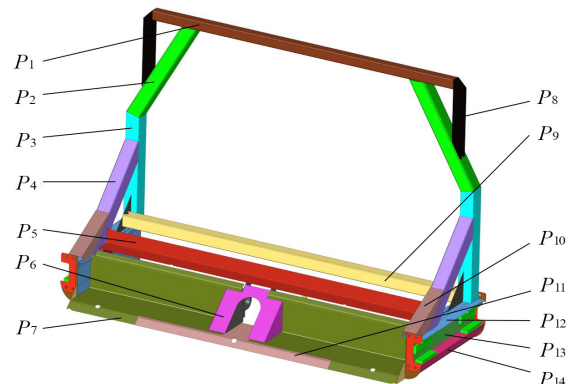


Fig. 11. Position of each design variable

### 2.5.2 Sensitivity analysis of design variables

Sensitivity analysis is a widely used tool in structural optimization, aimed at identifying design variables that significantly impact structural performance. The sensitivity value associated with changes in a design variable intuitively indicates both the magnitude and direction of its effect on performance, allowing for the rapid screening of critical design variables for optimization [27].

This analysis typically examines how the output response of a system is affected by its input parameters. For complex mathematical models, determining higher-order sensitivities can be challenging. Therefore, conventional sensitivity analysis focuses on the first-order partial derivatives of the design response with respect to the design variables. The mathematical expression is given by:

$$\text{sen} \left[ \frac{g(X)}{x_i} \right] = \frac{\partial g(X)}{\partial x_i}, \quad (1)$$

where  $g(X)$  is the system performance index,  $X$  is the system design parameter vector, and  $x_i$  is the  $i$ th parameter in the system design parameter vector.

The sensitivity of the 14 design variables in the ejector plate structure corresponding to the three performance indicators of mass, maximum von Mises stress and total deformation are calculated, as shown in Fig. 12, respectively.

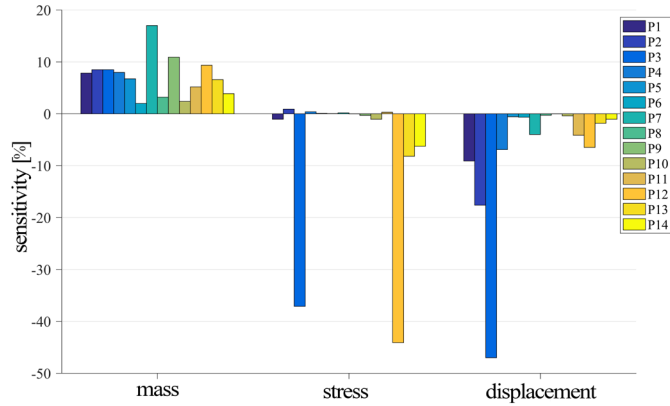


Fig. 12. Sensitivity of the candidate design variable

From Figure 12, we can see that:

1. The significance of all variables for total mass is positively correlated, with  $P_7$ ,  $P_9$ , and  $P_{12}$  having the greatest significance for total mass.
2.  $P_3$ ,  $P_{12}$ ,  $P_{13}$ , and  $P_{14}$  exhibit the most significant negative correlation with maximum von Mises stress, while the other variables show less significant correlations.
3. All variables show a negative correlation with total displacement.  $P_1$ ,  $P_2$ ,  $P_3$ ,  $P_4$ ,  $P_7$ ,  $P_{11}$  and  $P_{12}$  are most significantly negatively correlated with maximum deformation, while the remaining variables have a lesser impact.

Considering the sensitivity of each design parameter to the response value, 7 parameters are selected as design variables for the final size optimization. The initial values of each parameter and their allowable range of variation are presented in Table 2.

Table 2. Initial values and range of the ejector plate design variables [mm]

Design variables	Parameters	Original	Value range
Upper tube	$P_1$	3	2~4
Reinforced tube I	$P_2$	3.2	2~4.4
Side tube	$P_3$	3.2	2~4.4
Side steel tube	$P_4$	3.2	2~4.4
Bottom skeleton	$P_7$	5	4~6
Guide rail angle brace plate	$P_{12}$	3.2	2~4.4
Guide rail skeleton	$P_{13}$	4	3~5

## 2.6 Surrogate Model

A surrogate model is a mathematical representation constructed from a finite set of data obtained through computational or physical experiments. Complex models that require significant computational resources can be approximated using finite element-based models or less computationally intensive statistical models as surrogate models [28]. In optimization contexts, where evaluating objective and/or constraint functions demands considerable computational effort, a surrogate model effectively replace these functions [29]. The original model can be accurately predicted only if a highly precise surrogate model is developed.

The design of experiments (DOE) is a crucial step in creating a surrogate model, utilizing mathematical analyses such as probability theory and linear generation to identify reasonable discrete sample points. The distribution of these sample points within the design

space significantly influences the construction of the Kriging surrogate model, making the selection of an appropriate experimental design method critical for subsequent optimization. Commonly used experimental design methods include central composite design (CCD), Box-Behnken design (BBD), Latin hypercube design (LHS), and optimal space filling design (OSF). For this study, the Box-Behnken design method was chosen due to its advantages of requiring fewer trials and not necessitating the measurement of vertex points compared to other design methods.

### 2.6.1 Box-Behnken Design (BBD)

Using the upper tube thickness  $P_1$ , the reinforced tube I thickness  $P_2$ , the side tube thickness  $P_3$ , the side steel tube thickness  $P_4$ , the bottom skeleton thickness  $P_7$ , the rail angle brace thickness  $P_{12}$ , and the rail skeleton thickness  $P_{13}$  as independent variables, and the total mass ( $M$ ) of the ejector plate, the maximum displacement ( $D$ ), and the maximum von Mises stress ( $S$ ) as the evaluation indices, a total of 62 experimental samples and their corresponding response values were extracted, as shown in Table 3.

Table 3. Test samples and response values for BBD tests

Tests	$P_1$ [mm]	$P_2$ [mm]	$P_3$ [mm]	$P_4$ [mm]	$P_7$ [mm]	$P_{12}$ [mm]	$P_{13}$ [mm]	$M$ [kg]	$D$ [mm]	$S$ [MPa]
1	3	3.2	3.2	2	4	2	4	169.4	7.856	414.3
2	3	3.2	3.2	4.4	4	2	4	174.8	7.509	418.4
3	3	3.2	3.2	2	6	2	4	178.9	7.685	415.3
4	3	3.2	3.2	4.4	6	2	4	184.2	7.341	419.4
5	3	3.2	3.2	2	4	4.4	4	175.7	7.530	224.5
6	3	3.2	3.2	4.4	4	4.4	4	181.0	7.195	226.6
7	3	3.2	3.2	2	6	4.4	4	185.1	7.386	224.4
8	3	3.2	3.2	4.4	6	4.4	4	190.5	7.052	227.0
...	...	...	...	...	...	...	...	...	...	...
60	3	3.2	3.2	3.2	5	3.2	4	180.0	7.36	291.7
61	3	3.2	3.2	3.2	5	3.2	4	180.0	7.36	291.7
62	3	3.2	3.2	3.2	5	3.2	4	180.0	7.36	291.7

### 2.6.2 Kriging Surrogate Model

Kriging refers to a surrogate model based on Gaussian process modeling, which first originated in a geostatistical paper by Krige [30], and is now one of the most widely used surrogate modeling methods. The Kriging surrogate model can be expressed as follows:

$$y(x) = f(x) + Z(x), \quad (2)$$

where  $y(x)$  is an unknown function of the optimization objective,  $f(x)$  is a polynomial function on the variable  $x$ , and  $Z(x)$  is a stochastic function mainly used to correct the error of the global model.

The expression for  $f(x)$  is:

$$f(x) = \beta_0 + \sum_{i=1}^k \beta_i x_i + \sum_{i=1}^k \beta_{ii} x_i^2 + \sum_{i=1}^{k-1} \sum_{j=i+1}^k \beta_{ij} x_i x_j, \quad (3)$$

where  $k$  is the number of design variables, in this paper  $k=7$ ,  $\beta$  is the coefficient to be determined for each equation.

$Z(x)$  is a random function that follows a Gaussian normal distribution with zero mean.

$$E[Z(x)] = 0, \quad (4)$$

$$V[Z(x)] = \sigma^2. \quad (5)$$

$Z(x)$  creates a 'local' deviation that satisfies Eq. (4) with minimum variance to obtain the best valuation of the response surface of the kriging model interpolated to the  $N$  sample data points. The covariance matrix of is given by the following equation:

$$Cov[Z(x_i), Z(x_j)] = \sigma^2 R([r(x_i, x_j)]), \tag{6}$$

where  $R$  is the  $N \times N$  symmetric positive definite correlation matrix;  $r(x_i, x_j)$  is a Gaussian correlation function, which can represent the spatial correlation between any two sample points  $x_i$  and  $x_j$ . The expression is as follows:

$$r(x_i, x_j) = \exp\left(-\sum_{k=1}^M \theta_k |x_{ki} - x_{kj}|^2\right), \tag{7}$$

where  $\theta_k$  is the unknown parameter used for fitting;  $M$  is the number of design variables;  $x_{ki}$  and  $x_{kj}$  are the components of the  $k^{\text{th}}$  sampling point  $x_i, x_j$ .

Based on the unbiasedness of  $Z(x)$  and the minimum variance of the estimate, the relevant parameter  $\theta_k$  given by the maximum possible estimate, i.e. when  $\theta > 0$ , is derived to maximize the following equation:

$$A = -\frac{n_l \ln(\hat{\sigma}^2) + \ln|R(x)|}{2}, \tag{8}$$

where  $n_l$  is the number of response values,  $\hat{\sigma}^2$  is the variance estimate, and  $|R(x)|$  is the correlation value between the point to be measured and the sampling point. In other words, turn to find the minimum value.

$$\min_{x>0} \Psi(x) = |R(x)|^{\frac{1}{m}} \sigma^2. \tag{9}$$

### 2.6.3 Surrogate Model Accuracy Validation

The surrogate model may have some errors in the process of establishment, in order to verify the accuracy of the established surrogate model, the deterministic coefficient  $R^2$ , root mean square error ( $RMSE$ ) are introduced. The value of  $R^2$  ranges between  $[0, 1]$ , when the value of  $R^2$  tends to be closer to 1 and the value of  $RMSE$  tends to be closer to 1, they indicate that the accuracy of the fitted surrogate model is higher, and vice versa is lower. The formulas for calculating are as follows:

$$R^2 = 1 - \frac{\sum_{i=1}^n (y_i - \hat{y}_i)^2}{\sum_{i=1}^n (y_i - \bar{y}_i)^2}, \tag{10}$$

$$RMSE = \sqrt{\frac{1}{N} \sum_{i=1}^N (y_i - \hat{y}_i)^2}, \tag{11}$$

where  $y_i$  are true values of the test point,  $\hat{y}_i$  predicted values of the surrogate model for the test point,  $\bar{y}_i$  average of true values, and  $N$  number of sample points.

The fitting accuracy of the Kriging surrogate model and response surface methodology (RSM) surrogate model are obtained by solving Eq. (10) and Eq. (11), as shown in Fig. 13, and the specific values are shown in Table 4. It can be seen that the fitting accuracy values between the three objective functions of the ejector plate and the 7 key design variables are all greater than 0.90, while the coefficient of determination  $R^2$  of the general engineering requirements for the response surface model should not be less than 0.9 [31].

Table 4 shows the specific index values of the accuracy test results of each surrogate model.

Table 4. Accuracy of objective function

Performance	Kriging surrogate model		RSM surrogate model	
	$R^2$	$RMSE$	$R^2$	$RMSE$
mass	0.9505	0.0538	0.9468	0.0583
displacement	0.9659	0.0411	0.9503	0.0623
stress	0.9327	0.0601	0.9031	0.0736

The results show that both Kriging model and RSM model exhibit high accuracy, with  $R^2$  values exceeding 0.9 and  $RMSE$  values falling below 0.08. Overall, the Kriging model slightly exceeds the RSM model in terms of accuracy. Therefore, the Kriging surrogate model will be used for the subsequent multi-objective optimization.

## 2.7 Multi-Objective Optimization of the Ejector Plate

### 2.7.1 Mathematical Modeling

In order to achieve the purpose of lightweighting of the ejector plate, according to the Kriging surrogate model established by fitting, the mass of the ejector plate  $M$ , the maximum static deformation of the ejector plate skeleton  $D$  and the maximum von Mises stress  $S$  are taken as the optimization objective function, the maximum static deformation of the ejector plate skeleton  $D$  and the maximum von Mises stress  $S$  are taken as the constraints, and a total of 7 key dimensions of the ejector plate obtained from screening  $P_1 \sim P_4, P_7, P_{12}$  and  $P_{13}$  are taken as the independent variables of the objective function, so that the following multi-objective optimization mathematical model can be established. The multi-objective optimization mathematical model of ejector plate is as follows:

$$\begin{aligned} &\text{Find } x_i \ (i=1\sim 4, 7, 12, 13) \\ &\text{min: } \{M(x)\} \\ &\text{max: } \{D(x), S(x)\} \\ &\text{subject to } \begin{cases} D(x) \leq 10 \text{ mm,} \\ S(x) \leq 355 \text{ MPa,} \\ x_{i\text{min}} \leq x_i \leq x_{i\text{max}} \end{cases} \end{aligned} \tag{12}$$

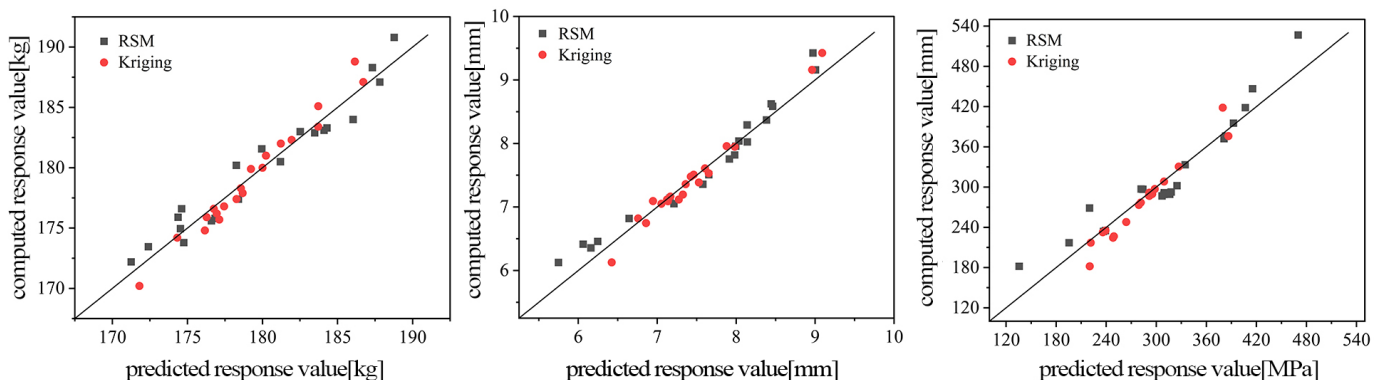


Fig.13. Surrogate model accuracy validation; a) mass b) displacement c) Von Mises stress

where  $x$  is the set of design variables;  $M(x)$  is the mass of the ejector plate [kg];  $D(x)$  is the displacement of the ejector plate skeleton [mm];  $S(x)$  is the von Mises stress of the ejector plate skeleton [MPa];  $x_{min}$  and  $x_{max}$  are the lower and upper bounds of each design variable.

### 2.7.2 Multi-Objective Optimization Using NSGA-II

NSGA-II is one of the most widely used and effective multi-objective evolutionary algorithms, originally proposed by Deb [25]. Unlike traditional genetic algorithms, NSGA-II introduces a fast non-dominated sorting method, an elite maintenance strategy, and an efficient congestion distance estimation process. These enhancements significantly accelerate iterative convergence, reduce computational complexity, and ensure population diversity [32].

In this paper, the NSGA-II algorithm is employed to address the multi-objective optimization problem. The population size is set to 120, with a maximum of 200 iterations. The algorithm utilizes a crossover probability of 0.9, a crossover distribution exponent of 10.0, and a mutation distribution exponent of 20.0.

## 3 RESULTS AND DISCUSSION

After 240,001 iterations, 742 non-dominated solutions were obtained. The Pareto front for the multi-objective optimization of the lightweight design of the ejector plate, produced by the NSGA-II algorithm, is shown in Fig. 14. In multi-objective optimization problems, the global optimal solution is typically not unique; instead, it consists of multiple optimal solutions, collectively known as the Pareto optimal solution set. After solving the developed response surface model, three sets of candidate solutions were identified, as presented in Table 5.

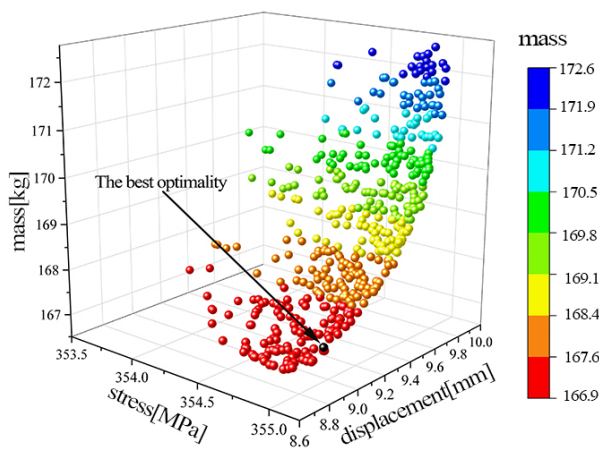


Fig. 14. Pareto solution set

Table 5 displays the optimized design parameters suggested by the software platform after problem resolution. Considering its superior performance in minimizing mass, displacement, and stress, Scheme 3 is identified as the most favorable design for the ejector plate. The

Table 5. Candidate combinations for design parameter optimization

No	Optimized design parameters							Optimal results		
	$P_1$ [mm]	$P_2$ [mm]	$P_3$ [mm]	$P_4$ [mm]	$P_7$ [mm]	$P_{12}$ [mm]	$P_{13}$ [mm]	$M$ [kg]	$D$ [mm]	$S$ [MPa]
1	2.4278	2.5407	2.6980	2.5852	4.1747	3.1341	3.5848	167.1	8.901	355.0
2	2.4408	2.5404	2.7123	2.5228	4.1790	3.1284	3.4678	167.0	8.862	355.0
3	2.4231	2.4693	2.7431	2.5534	4.1815	3.1013	3.5779	167.0	8.853	355.0

optimal design variables obtained after optimization were rounded for correction, and the finite element model of the ejector plate was re-analyzed for static characteristics based on this set of parameters. The performance indices corresponding to the design sizes of the ejector plate before and after optimization are summarized in Table 6.

Table 6. Comparison of the design variables before and after optimization

Design variables	Original	Optimal	Variation	Error
$P_1$ [mm]	3.0	2.3	-0.7	
$P_2$ [mm]	3.2	2.5	-0.7	
$P_3$ [mm]	3.2	3.0	-0.2	
$P_4$ [mm]	3.2	2.5	-0.7	
$P_7$ [mm]	5.0	4.0	-1.0	
$P_{12}$ [mm]	3.2	3.2	0	
$P_{13}$ [mm]	4	3.5	-0.5	
$M$ [kg]	180.0	169.1	-10.9	6.06 %
$D$ [mm]	7.36	8.20	+0.84	11.4 %
$S$ [MPa]	291.7	345.8	+54.1	18.5 %

As seen from Table 6, it demonstrates that the maximum displacement of the ejector plate skeleton has increased by 0.84 mm from 7.36 mm before optimization to 8.20 mm after optimization and the maximum equivalent stress of the ejector plate skeleton has increased by 54.1 MPa from 291.7 MPa before optimization to 345.8 MPa after optimization. Although both indicators have increased, they meet the design requirements. After optimization, the ejector plate's total mass decreased from 180 kg to 169.1 kg, achieving a reduction of 10.9 kg (6.06 %) compared to the original design. The optimization effect is clear, achieving the intended optimization goals. The effectiveness of the proposed scheme has been validated in actual production, as illustrated in Fig. 15. The mass of the ejector plate has been reduced, material utilization has improved, and safety is maintained.



Fig. 15. Application of the ejector plate optimization

## 4 CONCLUSIONS

This work presents an innovative lightweight design framework for rear-loader garbage truck ejector plates, which integrates multi-objective optimization algorithms with surrogate modeling techniques to achieve balanced improvements in structural performance and economic efficiency. Through systematic optimization, the final design demonstrates a total mass reduction to 169.1 kg (6.06 % lighter than the original design) while satisfying all operational constraints. The main findings can be summarized as follows:

- Comparative analysis of surrogate modeling approaches shows that the Kriging model exhibits superior prediction accuracy compared to the RSM model, particularly in capturing the response characteristics of the ejector plate system.
- The implementation of global sensitivity analysis allows effective identification of critical design parameters that have dominant influences on key performance indicators, thereby reducing computational costs by reducing experimental design parameters.
- The NSGA-II evolutionary algorithm is shown to be effective in generating Pareto optimal solutions for push plate parameters, achieving convergence within 200 generations while maintaining solution diversity through tournament selection and simulated binary crossover mechanisms.

In particular, the developed methodology demonstrates strong scalability and provides a generalized framework for the optimization of various load-bearing components in heavy-duty vehicles, including but not limited to chassis structures and actuator systems. Future work should focus on experimental validation of optimized designs under real-world operating conditions and extension.

## References

- [1] Mostafayi Darmian, S., Moazzeni, S., Hvattum, L.M. Multi-objective sustainable location-districting for the collection of municipal solid waste: Two case studies. *Comput Ind Eng* 150 106965 (2020) DOI:10.1016/j.cie.2020.106965.
- [2] Wan, H., Ma, J., Yu, Q., Sun, G., He, H., Li, H. Modeling and optimization of multi-model waste vehicle routing problem based on the time window. *J Database Manag* 34 1-16 (2023) DOI:10.4018/jdm.321543.
- [3] Negreanu, G.P., Voicu, G., Lazea, M., Constantin, G.-A., Stefan, E.-M., Munteanu, M.-G., et al. Finite element analysis of the compaction plate from a garbage truck. *E3S Web Conf* 180 04006 (2020) DOI:10.1051/e3sconf/202018004006.
- [4] Zheng, X., Guo, J., Li, S. Design and mechanical analysis of the loading mechanism of the back-loading garbage truck. *IOP Conf Ser Mater Sci Eng* 612 032043 (2019) DOI:10.1088/1757-899x/612/3/032043.
- [5] Luo, L., Li, X., Yuan, M. (2023). Lightweight optimization of garbage collection truck manipulator based on parametric modelling. *J Phys Conf Ser* 2587 012032 DOI:10.1088/1742-6596/2587/1/012032.
- [6] Cavazzuti, M., Baldini, A., Bertocchi, E., Costi, D., Torricelli, E., Moruzzi, P. High performance automotive chassis design: A topology optimization based approach. *Struct Multidiscip Optim* 44 45-56 (2011) DOI:10.1007/s00158-010-0578-7.
- [7] Li, S., Zhou, D., Pan, A. Integrated lightweight optimization design of wall thickness, material, and performance of automobile body side structure. *Struct Multidiscip Optim* 67 95 (2024) DOI:10.1007/s00158-024-03810-1.
- [8] Yu, L., Gu, X., Qian, L., Jiang, P., Wang, W., Yu, M. Application of tailor rolled blanks in optimum design of pure electric vehicle crashworthiness and lightweight. *Thin-Walled Struct* 161 107410 (2021) DOI:10.1016/j.tws.2020.107410.
- [9] Del Pero, F., Berzi, L., Antonacci, A., Delogu, M. Automotive lightweight design: Simulation modeling of mass-related consumption for electric vehicles. *Machines (Basel)* 851 (2020) DOI:10.3390/machines8030051.
- [10] Xu, X., Chen, X., Liu, Z., Xu, Y., Zhang, Y. Reliability-based design for lightweight vehicle structures with uncertain manufacturing accuracy. *Appl Math Model* 95 22-37 (2021) DOI:10.1016/j.apm.2021.01.047.
- [11] Shangguan, Y., Wang, W., He, A., Ma, W., Tian, H. Lightweight design for the aluminum alloy-carbon fiber hybrid structure of the EMU car body. *J Mech Sci Technol* 37 6441-6452 (2023) DOI:10.1007/s12206-023-1116-z.
- [12] Fu, L., Zhang, S., Qiu, P., Xiao, H., Deng, B., Lu, X. Optimization of clinching joint process with preforming between ultra-high-strength steel and aluminum alloy sheets. *Metals (Basel)* 14 767 (2024) DOI:10.3390/met14070767.
- [13] Dogan, O., Karpat, F., Yuce, C., Kaya, N., Yavuz, N., Sen, H. A novel design procedure for tractor clutch fingers by using optimization and response surface methods. *J Mech Sci Technol* 30 2615-2625 (2016) DOI:10.1007/s12206-016-0522-x.
- [14] Zhang, Y., Shan, Y.C., Liu, X.D., He, T. Integrated shape-morphing and surrogate model-assisted multi-objective structural optimization of an automobile wheel made of lightweight materials to improve its impact resistance. *Eng Optim* 56, 1972-1998 (2023) DOI:10.1080/0305215x.2023.2291481.
- [15] Wang, Z.H., Zhang, T.Q., Zhang, Y., Jiang, Z.P., Wu, F.H. Shape optimization method for wheel rim of automobile wheels based on load path analysis. *P I Mech EnC-J Mech* 237 267-280 (2023) DOI:10.1177/09544062221119360.
- [16] Cheng, M.-Y., Prayogo, D., Wu, Y.-W., Lukito, M.M. A hybrid harmony search algorithm for discrete sizing optimization of truss structure. *Autom Constr* 69 21-33 (2016) DOI:10.1016/j.autcon.2016.05.023.
- [17] Goldberg, D.J.O. *Genetic Algorithms in Search, Optimization and Machine Learning* (1989). Addison-Wesley Professional, Boston.
- [18] Paz, J., Díaz, J., Romera, L., Costas, M. Crushing analysis and multi-objective crashworthiness optimization of gfrp honeycomb-filled energy absorption devices. *Finite Elem Anal Des* 91 30-39 (2014) DOI:10.1016/j.finel.2014.07.006.
- [19] Velea, M.N., Wennhage, P., Zenkert, D. Multi-objective optimisation of vehicle bodies made of frp sandwich structures. *Comp Struct* 111 75-84 (2014). DOI:10.1016/j.compstruct.2013.12.030.
- [20] Duan, L., Li, G., Cheng, A., Sun, G., Song, K. Multi-objective system reliability-based optimization method for design of a fully parametric concept car body. *Eng Optim* 49 1247-1263 (2017) DOI:10.1080/0305215x.2016.1241780.
- [21] Jiang, R., Jin, Z., Liu, D., Wang, D. (2021). Multi-objective lightweight optimization of parameterized suspension components based on NSGA-II algorithm coupling with surrogate model. *Machines (Basel)* 9 107 DOI:10.3390/machines9060107.
- [22] Xie, C., Wang, D., Wang, S., Kong, D., Du, C. A performance-driven lightweight optimization method for material-structure coupling design of cab. *Struct Multidiscip Optim* 67 12 (2024) DOI:10.1007/s00158-023-03730-6.
- [23] Qian, J., Yi, J., Cheng, Y., Liu, J., Zhou, Q. A sequential constraints updating approach for kriging surrogate model-assisted engineering optimization design problem. *Eng Comput* 36 993-1009 (2020) DOI:10.1007/s00366-019-00745-w.
- [24] Kaintura, A., Spina, D., Couckuyt, I., Knockaert, L., Bogaerts, W., Dhaene, T. A Kriging and stochastic collocation ensemble for uncertainty quantification in engineering applications. *Eng Comput* 33 935-949 (2017) DOI:10.1007/s00366-017-0507-0.
- [25] Deb, K., Pratap, A., Agarwal, S., Meyarivan, T. A fast and elitist multiobjective genetic algorithm: NSGA-II. *IEEE Trans Evol Comput* 6 182-197 (2002) DOI:10.1109/4235.996017.
- [26] Zienkiewicz, O.C., Zhu, Z.J. The superconvergent patch recovery and a posteriori error estimates. Part 2: Error estimates and adaptivity. *Int J Numerical Meth Eng* 33 1365-1382 (1992) DOI:10.1002/nme.1620330703.
- [27] Kim, S.Y. Constrained sensitivity filtering technique for topology optimization with lower computational expense. *Int J Numer Meth Eng* 124 4075-4096 (2023). DOI:10.1002/nme.7301.
- [28] Kudela, J., Matousek, R. Recent advances and applications of surrogate models for finite element method computations: A review. *Soft Comput* 26 13709-13733 (2022) DOI:10.1007/s00500-022-07362-8.
- [29] Juliani, M.A., Gomes, W.J.S. An efficient Kriging-based framework for computationally demanding constrained structural optimization problems. *Struct Multidiscip Optim* 65 4 (2022) DOI:10.1007/s00158-021-03095-8.
- [30] Krige, D.G. A statistical approach to some basic mine valuation problems on the witwatersrand. *J Chem Metall Min Soc S Afr* 52 119-139 (1951).
- [31] Van, A.-L., Nguyen, T.-C., Bui, H.-T., Dang, X.-B., Nguyen, T.-T. Multi-response optimization of gtaw process parameters in terms of energy efficiency and quality. *Stroj vestn-J Mech E* 70 259-269 (2024) DOI:10.5545/sv-jme.2023.890.
- [32] Huang, W., Huang, J., Yin, C. Optimal design and control of a two-speed planetary gear automatic transmission for electric vehicle. *Appl Sci (Basel)* 10 6612 (2020) DOI:10.3390/app10186612.

**Acknowledgements** This work was supported by the National Natural Science Foundation of China under Grant (51875494).

Received 2024-10-05, revised 2025-04-07, 2025-04-30,  
accepted 2025-05-13 as Original Scientific Paper.

**Data availability** The data that support the findings of this study are available from the corresponding author upon reasonable request.

**Author contributions** Fu-sheng Ding: methodology, formal analysis, validation, writing – original draft; Hong-ming Lyu: supervision, project administration, methodology, review & editing; Jun Chen: conceptualization, methodology, review & editing. Hao-ran Cao: methodology, formal analysis, data curation. Lan-xiang Zhang: formal analysis, data curation. All authors have contributed significantly to this work and thoroughly reviewed and approved the final version of the manuscript.

**AI-Assisted writing** AI-based tools were employed solely to enhance the readability and grammatical accuracy of the manuscript.

## Večkriterijska optimizacija zasnove iztisne plošče za smetarska vozila z zadenjskim nakladanjem

**Povzetek** V delu je predstavljena večkriterijska optimizacija zasnove iztisne plošče, ključne komponente smetarskih vozil z zadenjskim nakladanjem, z namenom ohranjanja trdnosti ob hkratni optimizaciji mase. Zasnovan je bil parametrični model s končnimi elementi iztisne plošče, pri čemer so bili cilji optimizacije usmerjeni v zmanjšanje mase, maksimiranje omejitev deformacij ter zmanjšanje maksimalne von Misesove napetosti. Z analizo občutljivosti je bilo identificiranih sedem ključnih spremenljivk. Sistematična zasnova parametrov je bila izvedena s pomočjo Box-Behnkenovega načrtovanja eksperimentov (BBD), ciljna funkcija pa je bila približana s Križingovim nadomestnim modelom, katerega učinkovitost je bila primerjana z metodo odzivne površine (RSM). Za določitev optimalne rešitve je bil uporabljen večkriterijski genetski algoritem NSGA-II, ki omogoča lahkotnejšo zasnovo ob izpolnjevanju vseh strukturnih zahtev. Rezultati kažejo, da je možno maso iztisne plošče smetarskega vozila z zadenjskim nakladanjem z optimizacijo zmanjšati za 6,06 %, pri čemer so izpolnjeni kriteriji trdnosti in deformacij. Ta izboljšava ne poveča le učinkovitosti transporta odpadkov, ampak tudi zmanjša proizvodne stroške in izboljša izkoriščenost gradiv.

**Ključne besede** smetarsko vozilo, iztisna plošča, večkriterijska optimizacija, NSGA-II, Križing